



Are the Norwegian mountains compensated by a mantle thermal anomaly at depth?

Christophe Pascal*, Odleiv Olesen

NGU, Geological Survey of Norway, N-7491 Trondheim, Norway

ARTICLE INFO

Article history:

Received 27 June 2008

Received in revised form 8 December 2008

Accepted 9 January 2009

Available online 21 January 2009

Keywords:

Bouguer anomalies

Heat flow

Isostasy

Asthenospheric diapir

ABSTRACT

The Norwegian mountains or Scandes represent a long mountain range stretching from southern Norway to the Arctic and is characterised by a rugged topography and peaks up to 2.5 km high. The origin of this mountain chain far away from any plate boundary remains a matter of passionate debates inside the geoscientific community. Hot mantle “fingers” originating from the Iceland Plume, impacting the base of the Scandinavian lithosphere and creating asthenospheric diapirs is one of the most accepted hypotheses for explaining Cenozoic uplift in Norway. In order to test this hypothesis we conducted integrated gravity and thermal modelling. We used the dense NGU gravity grid (i.e. one measurement every ~3 km) and modelled the depth extent and the mass deficit associated to the compensating loads located below the southern Scandes. Assuming that the density deficit below the Scandes is purely thermal in origin, thermal modelling allowed for testing the magnitude of the potentially associated temperature anomaly and its impact on surface heat flow. Recently acquired heat flow data were used in order to constrain the results from the thermal modelling. The results of our integrated geophysical modelling rule out the possibility that the present-day topography of the southern Scandes is compensated by a deep-seated asthenospheric diapir. However, our modelling does not exclude that thermal processes in the deep mantle could have initiated or assisted recent uplift of the southern Scandes.

© 2009 Elsevier B.V. All rights reserved.

1. Introduction

The Norwegian mountains (i.e. Scandinavian mountains or Scandes) represent a long mountain range stretching for more than 1400 km through most of Norway and parts of central and northern Sweden (Fig. 1a) and has peaks up to ~2.5 km. The Scandes are traditionally divided into two dome-like areas (i.e. southern and northern Scandes) separated by a central area with less pronounced topography. The Scandes involve a variety of geomorphological features but are mostly dominated by flat-lying plateaux located at different altitudes (Lidmar-Bergström and Näslund, 2002). After the topography itself the gravity field is probably the best constrained geophysical dataset in Fennoscandia and in particular in Norway (Fig. 1b). Already noted by many authors (e.g. Balling, 1980; Olesen et al., 2002; Rohrman et al., 2002), the Scandes found their counterpart in the Bouguer gravity field in the form of pronounced lows (i.e. down to –100 mGal), suggesting isostatic compensation by mass deficit below the mountain range.

The formation of the Scandes is being discussed for more than one century, since Reusch (1901, 1903) proposed that the plateaux were remnants of a peneplain formed close to sea-level. The massive influx of Cenozoic clastic sediments revealed by a systematic exploration of nearby offshore regions in the second half of the 20th century (e.g. Doré, 1992; Riis, 1996; Faleide et al., 2002) added support to the

hypothesis that the Scandes are relatively young mountains. Evidence for a recent uplift event in Scandinavia has been growing during the past decades (Japsen and Chalmers, 2000) but to date no consensus on its causes has been reached yet.

The origin of the Scandes mountain chain far away from any plate boundary remains a matter of passionate debates inside the geoscientific community and various models have been advanced. A non-exhaustive list of invoked causes includes: opening of the NE Atlantic (Torske, 1972), isostatic response to glacial erosion (Doré, 1992; Riis and Fjeldskaar, 1992), pre-subduction instability (Sales, 1992), intraplate stresses (Cloetingh et al., 1990), mantle convection (Bannister et al., 1991), climate deterioration and sea-level changes (Eyles, 1996), small-scale convection (Stuevold and Eldholm, 1996), rift-shoulder uplift (Doré, 1992; Redfield et al., 2005), asthenospheric diapirism (Rohrman and van der Beek, 1996; Rohrman et al., 2002), migrating phase boundaries (Riis and Fjeldskaar, 1992), serpentinisation (Skelton and Jakobsson, 2007) and more recently modification of the Caledonian topography (Nielsen et al., 2009). As a rule at thumb, model abundance reflects data scarcity. The most accepted model and probably the most satisfactory one in terms of accounting for most of the observations, is the asthenospheric diapir model advanced by Rohrman and van der Beek (1996).

The aim of the present contribution is to test the limits of Rohrman and van der Beek's hypothesis by means of integrated modelling of high-resolution gravity data with modern heat flow data. We firstly summarise the theoretical background and the implications of the asthenospheric diapir model. In the following we model the long-

* Corresponding author.

E-mail address: Christophe.pascal@ngu.no (C. Pascal).

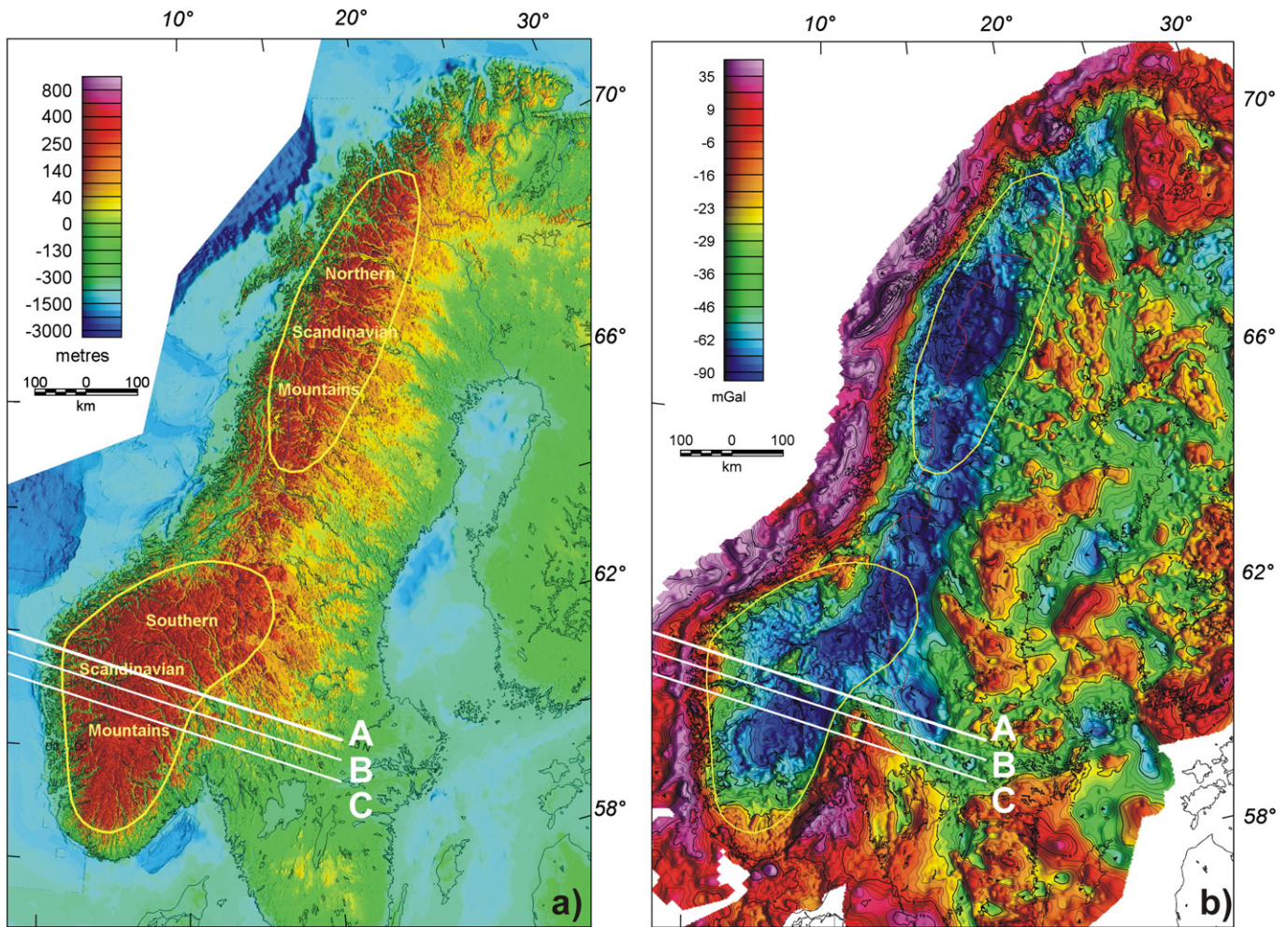


Fig. 1. a) Topography (Dehls et al., 2000) and b) Bouguer gravity anomalies of Fennoscandia (Skilbrei et al., 2000, Korhonen et al., 2002). Note the spatial correlation between the most pronounced gravity lows and the location of the Scandinavian Mountains or Scandes.

wavelength (i.e. associated to the compensating masses below the mountains) signal of the Bouguer gravity field in southern Norway, in order to constrain the depth of the assumed asthenosphere body and its density deficit or, conversely, its temperature excess. The predictions are then tested against thermal data and the outcomes of our work are discussed.

2. The asthenospheric diapir model

The asthenospheric diapir model (Fig. 2) involves impingement of anomalously hot asthenosphere at the base of cold cratonic lithosphere (Rohrman and van der Beek, 1996; Rohrman et al., 2002). According to the model, the hot asthenosphere takes its origin in the Iceland hotspot emplaced into the Norwegian–Greenland Sea at ~30 Ma (Lawver and Müller, 1994). Hot material travels through a thin asthenosphere layer before meeting cold cratonic lithosphere. The contrast in temperature (i.e. viscosity) between the two produces a Rayleigh–Taylor instability. This process is similar to the one that leads to the formation of thunderclouds. Finally the rise of the asthenospheric diapir creates isostatic uplift of the surface. Rohrman and van der Beek (1996) invoke two cases. In the first case, the diapir has reached relatively shallow levels in the lithosphere and subsequent decompression melting results in volcanism at the surface (e.g. Spitsbergen). In the second case, which would be representative for the Scandes, the asthenospheric diapir is still located at great depths present-day and, therefore, its associated thermal effects have not reached the surface yet.

The asthenospheric diapir model is probably the most elegant one while reconciling different pieces of the puzzle. It accounts for both the amount (i.e. 1–2 km) and the timing (i.e. mostly Neogene) of uplift and integrates various geological and geophysical observations in a coherent scheme (Rohrman et al., 2002). The main conclusions derived by Rohrman and van der Beek (1996) are that the top of the diapir is located at ~100 km depth, its vertical extent is ~100 km, its radius 100–150 km and the temperature contrast between the hot asthenosphere and the cold lithosphere is ~400 °C (Fig. 2). Bearing in mind these numerical values, we propose to evaluate the asthenospheric diapir model.

3. Integrated gravity-thermal models of the southern Scandes

3.1. Constraints from gravity modelling

We focused our study on the southern Scandes and used the high-resolution (i.e. one measurement every ~3 km) gravity database at NGU (Skilbrei et al., 2000). We selected to model Bouguer anomalies along three NW–SE profiles across the middle of the southern Scandes (Fig. 1). Ideally we should have filtered the Bouguer anomalies in order to retain the signal produced by the deep sources compensating for the observed topography. However, short-wavelength anomalies, related to shallow sources, can be easily detected when comparing the three profiles between them. For example, the high-density mafic granulites and gabbros of the Jotun Nappe Complex (Milnes and Koestler, 1985; Skilbrei, 1990) add a positive gravity component at

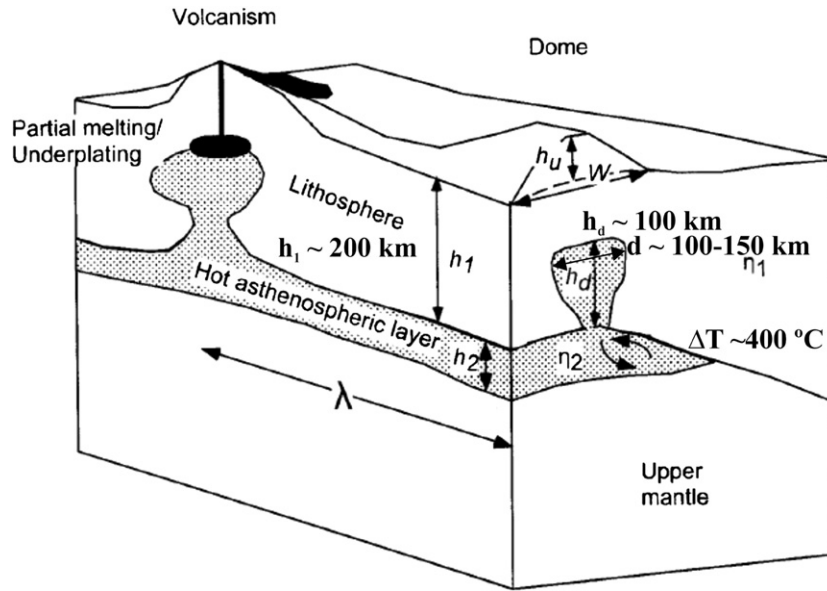


Fig. 2. The asthenospheric diapir model: interaction between anomalously hot asthenosphere and cold cratonic lithosphere produces a Rayleigh–Taylor instability, penetration of hot asthenosphere into mantle lithosphere and subsequent uplift of the Earth's surface (redrawn from Rohrman and van der Beek, 1996).

~300 km on Profile A that is absent on Profiles B and C (Figs. 1b and 3). Similarly, the effects related to the crustal structure of the Permian Oslo Graben (e.g. Ebbing et al., 2005) are seen as a progressive increase in gravity gradients between 400 and 500 km when moving southwards from Profiles A to C (Fig. 3). In brief, because the first-order characteristics of the gravity signal associated to the compensating masses is apparent in Fig. 3, we preferred not to complicate our analysis. The aim of our modelling was to find the nature and depth of the sources that reproduce a gravity signal consistent with the one suggested by the cloud of gravity data. The gravity response was calculated using the commercial GM-SYS software from Geosoft Inc. based on the two and one-half-dimensional modification by Rasmussen and Pedersen (1979) of the original forward 2D algorithm by Talwani et al. (1959). GM-SYS is an interactive $2^{3/4}D$ gravity and magnetic modelling program using a method of summing irregular polygons.

Firstly we placed at 100 km depth a 100 km wide body and tested different density contrast values with respect to the neighbouring rocks (Fig. 4). Compared to the mushroom shape that is expected to characterise an asthenospheric diapir, the shape of the body is simplified but represents a reasonable approximation for the purposes of the present study. Our analysis shows that a density reduction between the lithosphere and the hot asthenosphere of -50 kg/m^3 , which would correspond to a reasonable value of $\sim 3250 \text{ kg/m}^3$ for the

density value of the asthenosphere, produces a very smooth gravity signal unlikely to be detected. Increasing the density contrast to -100 kg/m^3 increases notably the amplitude of the signal and its gradient but is far from satisfying the shape of the gravity low as it is suggested by the cloud of data points. Apparently a density contrast higher than this latter value and close or equal to -200 kg/m^3 would meet our requirements (Fig. 4). It is straightforward to derive the temperature change, ΔT , needed to create a given density contrast, $\Delta \rho$, using:

$$\Delta T = -\Delta \rho / (\rho_l \cdot \alpha_v) \quad (1)$$

where ρ_l is mantle lithosphere average density and α_v is the volume coefficient of thermal expansion equal to $4 \cdot 10^{-5} \text{ K}^{-1}$ for most mantle rocks at temperatures in the range 1000–1600 °C (Poudjom Djomani et al., 2001). This simple analysis shows that gravity model a) in Fig. 4 results in a realistic ΔT value (i.e. ~ 400 °C) similar to the one proposed by Rohrman and van der Beek (1996). This value implies a temperature of ~ 1400 °C for the diapir assuming mean temperatures around 1000 °C for the deepest levels of the lithosphere. However, more significant density contrasts, which are obviously needed in order to fit the observed gravity, would result in unrealistically high ΔT values (i.e. $\Delta T > 750$ °C, Fig. 4), corresponding to temperatures higher than, at least, 1750 °C for the assumed diapir. This value exceeds

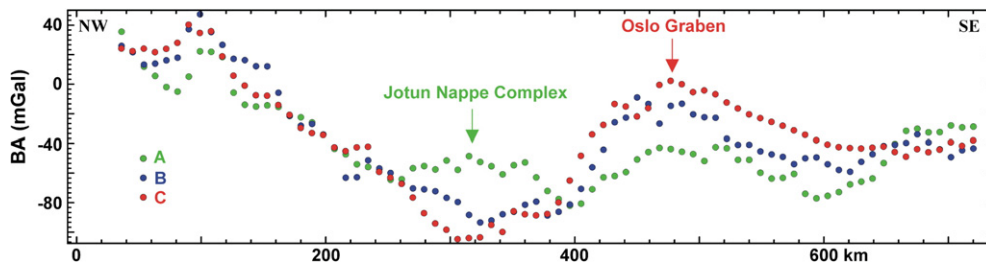


Fig. 3. Bouguer anomalies (total field) along Profiles A, B and C. The short-wavelength signal from relatively shallow sources (e.g. Jotun Nappes Complex and Oslo Graben, see text) can be isolated allowing for a first-order separation of the signal related to the compensating masses below the southern Scandes. See Fig. 1 for location of the profiles.

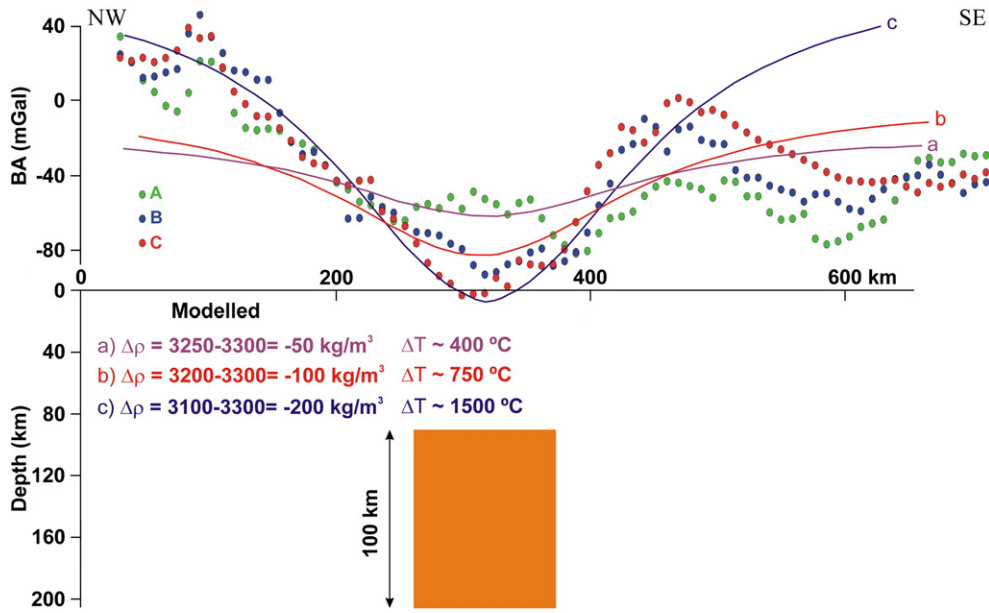


Fig. 4. Gravity modelling assuming an asthenospheric diapir at 100 km depth and as a function of density contrast (i.e. temperature contrast) between the diapir and surrounding lithosphere.

by ~150 °C maximum temperatures estimated for thermal anomalies in the upper mantle (e.g. Goes et al., 2004). In brief, this first modelling exercise demonstrates that, in order to match the observed gravity low, the asthenospheric diapir cannot be located at great depths below the surface. Note that this conclusion gains even more support if a lower α_V value is considered (e.g. $3.5 \cdot 10^{-5} \text{ K}^{-1}$, Afonso et al., 2005).

Alternatively, the lithosphere might have been thinner than proposed originally in the asthenospheric diapir model (Fig. 2) and the diapir could be at shallower depths than anticipated. We calculated the gravity effect placing the diapir at different depths. A reasonable fit between observed and modelled gravity is obtained only if we assume that the diapir has reached relatively shallow depths (i.e. ~40 km.), close to the Moho (Kinck et al., 1993). It appears that a density contrast between $\Delta\rho = -50 \text{ kg/m}^3$ and $\Delta\rho = -100 \text{ kg/m}^3$

would reproduce reasonably well the observed gravity low (Fig. 5). This implies that the diapir/lithosphere temperature contrast has to be between $\Delta T = 400 \text{ }^\circ\text{C}$ and $\Delta T = 750 \text{ }^\circ\text{C}$ (Fig. 5).

3.2. First-order thermal models

We explore now the consequences for surface heat flow assuming that the diapir is located at 40 km depth and ΔT is between 400 and 750 °C. We used information from newly acquired heat flow data in Norway onshore. A detailed description of this brand new dataset is beyond the scope of the present paper and is included in a Ms recently submitted to Tectonophysics (Slagstad et al., in revision). We briefly summarise some of its aspects relevant for our study. The heat flow database in southern Norway involves currently nine measurements

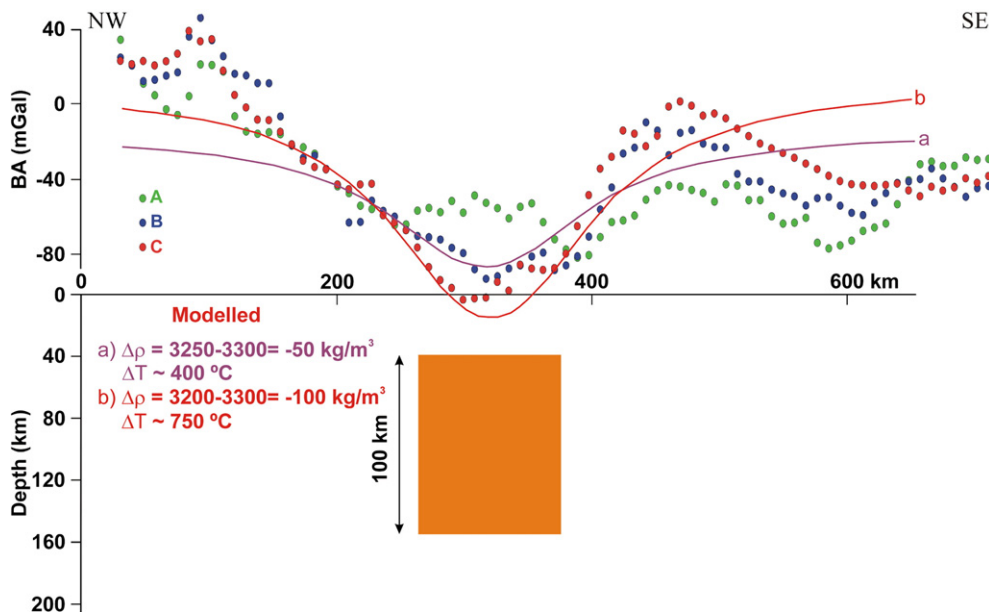


Fig. 5. Gravity modelling assuming an asthenospheric diapir just below the Moho at 40 km depth.

made in boreholes down to ~1000 m. The main outcome of the heat flow study is that surface heat flow in southern Norway is higher by 15 mW/m² than previously claimed (Hänel et al., 1979) and typical values after corrections are 58 ± 12 mW/m².

Bearing in mind this constraint we computed the expected evolution of surface heat flow as function of time after emplacement of a mantle diapir at 40 km depth, using the classical “1D slab” equation (Carslaw and Jaeger, 1959; Bodell and Chapman, 1982):

$$\Delta q(t) = \frac{k\Delta T}{d} \left\{ 1 + 2 \sum_{n=1}^{\infty} \cos(n\pi) \exp \left[\frac{-n^2 \pi^2 \kappa t}{d^2} \right] \right\} \quad (2)$$

where k is thermal conductivity, κ thermal diffusivity (Table 1), d depth to the diapir's top and $t > 0$ is time after application of the temperature change ΔT . Our analysis shows that 30 Myr after emplacement of the diapir, surface heat flow has already increased by 25 to 46 mW/m² depending on ΔT (Fig. 6). Note that these values represent lower bounds. One should expect an additional and significant part of heat to be transported by advection as magmas travel to the surface.

According to the offshore stratigraphic record (e.g. Riis, 1996) and apatite fission-track analyses (Rohrman et al., 1995, 2002), uplift and denudation in southern Norway began at least 30 Myr ago. Minimum continental heat flow is ~40 mW/m² in steady-state conditions and in a regional sense (Nyblade and Pollack, 1993). We thus consider this latter value as a minimum estimate for the pre-uplift heat flow and assume that the additional ~20–30 mW/m² observed in southern Norway are sourced by the hot diapir. If an asthenospheric diapir would have created the topography 30 Myr ago and would compensate it today, the results in Fig. 6 show that ΔT has to be lower than 500 °C (i.e. $\Delta q < 30$ mW/m²) in order to explain the present-day surface heat flow (i.e. 58 ± 12 mW/m²). ΔT values higher than 500 °C would result in surface heat flow values higher than 70 mW/m² for $t > 30$ Myr (Fig. 6), well above observed values. Our gravity modelling shows that modest ΔT values (i.e. close to 400 °C, Fig. 5) do not produce sufficient density reduction of the mantle that would, in turn, explain the observed gravity low. This first-order analysis suggests that a hot asthenospheric diapir is merely not supporting the topography of the southern Scandes.

3.3. 2-D finite-element thermal modelling

The analytical “1D slab” approach, very often used in the literature, represents a crude simplification of the actual case. In order to test our previous results, we modelled by means of finite element methods, the 2D transient response of the lithosphere after emplacement of a hot diapir. The model setup is shown in Fig. 7 and model parameters are given in Table 1. We assumed a sudden raise in temperatures at the location of the diapir at $t = 0$ and let the system evolve. In the present case, the thermal structure of the lithosphere is modelled in a much more detail than in the analytical approach. Consequently, we found it more accurate to use the temperature of the diapir (i.e. T_d) as modelling parameter and not the average temperature contrast between the diapir

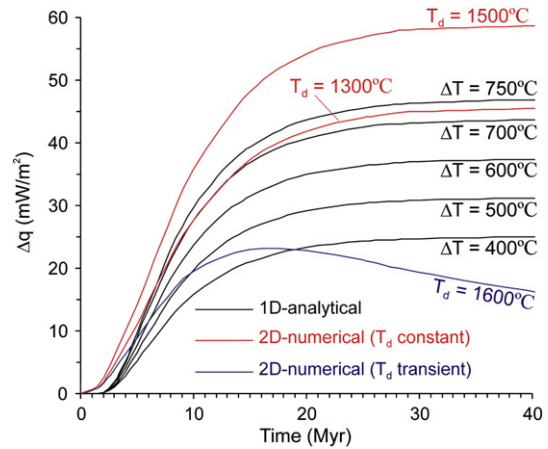


Fig. 6. Evolution of surface heat flow vs time after emplacement of the asthenospheric diapir at 40 km depth. Black curves represent 1-D analytical solutions where ΔT is the temperature contrast between the asthenospheric diapir and the lithosphere. Red curves represent 2-D numerical solutions where T_d is diapir temperature and is kept constant. The blue curve represents a 2-D numerical solution where T_d is fixed at $t = 0$ but evolves by heat diffusion (i.e. cooling) afterwards. (For interpretation of the references to colour in this figure legend, the reader is referred to the web version of this article.)

and the lithosphere (i.e. ΔT). Note that adiabatic cooling of the asthenosphere is negligible in the present case.

In the first modelled case we set a temperature of $T_d = 1500$ °C for the diapir and maintained it constant through time (Fig. 6). This latter value represents a mantle thermal anomaly with average temperatures (e.g. Goes et al., 2004) but already results in an increase in surface heat flow of more than 55 mW/m², 20 Myr after its application (Fig. 6). Even if we model an unrealistically low value of $T_d = 1300$ °C (i.e. corresponding to “normal” asthenosphere), the increase in surface heat flow after 20 Myr reaches more than 40 mW/m² (Fig. 6). Obviously the “1D slab” approach underestimates heat flow values although it reproduces a similar time-evolution for the surface heat flow. Additional tests, which for the sake of clarity we avoided in Fig. 6, show that the numerical solutions for $T_d = 1300$ °C and $T_d = 1500$ °C are well reproduced using Eq. (2) and taking $\Delta T \sim 725$ °C and $\Delta T \sim 940$ °C respectively. These latter values correspond well to the maximum temperature contrasts in the numerical models at 40 km depth and $t = 0$ (i.e. Moho temperature by 540 °C). This shows that the underestimation in surface heat flow values using the analytical approach is the direct consequence of averaging lithosphere temperatures which, in turn, results in ΔT values lower than those predicted by the numerical model. We may also note that the finite-element model predicts the onset of increase in surface heat flow 2 Myr earlier than the analytical solution. Nevertheless, the obvious conclusion from the present modelling tests is that the emplacement of a mantle diapir at 40 km depth 30 Myr ago is unlikely, because it would have produced much higher present-day surface heat flow values than actually measured.

It is, however, doubtful that the intruded diapir could maintain a constant temperature with time. The very last numerical modelling

Table 1
Parameters used in this study.

Quantity	Symbol	Value
Volumetric thermal expansion ^a	α_v	$4 \cdot 10^{-5} \text{ K}^{-1}$
Crust thermal conductivity ^b	k	2.5 W/m/K
Crust thermal diffusivity ^b	κ	$0.9 \cdot 10^{-6} \text{ m}^2/\text{s}$
Crustal heat generation ^c	A_0	0.35 $\mu\text{W}/\text{m}^3$
Mantle thermal conductivity ^c	k'	3.5 W/m/K
Mantle thermal diffusivity ^c	κ'	$1 \cdot 10^{-6} \text{ m}^2/\text{s}$

^a Analytical calculations only.

^b In both analytical and numerical calculations.

^c Numerical calculations only.

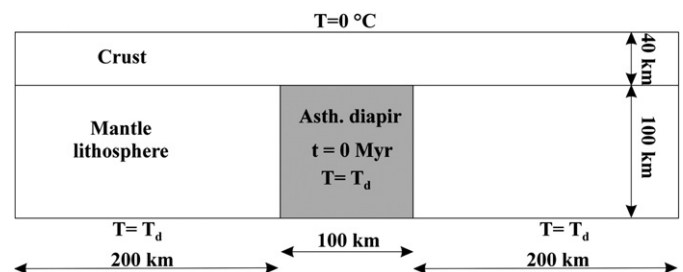


Fig. 7. Set up of the 2D finite-element model. T_d is diapir temperature.

test consists in exploring the effect of cooling of the asthenospheric diapir on the evolution of surface heat flow and mantle densities. We used similar modelling parameters than previously but allowed diapir temperatures to evolve following 2D heat diffusion. We report here only one simulation where T_d was set to its maximum allowed value

of 1600 °C (i.e. mantle thermal anomaly of + 300 °C, Goes et al., 2004) at $t = 0$. The cooling of the diapir, following its assumed fast intrusion into the lithosphere, is rapid in particular at shallow depths (Figs. 8 and 9a). Compared to previous modelling results the surface heat flow signal is drastically reduced (Fig. 6) and decays after having reached

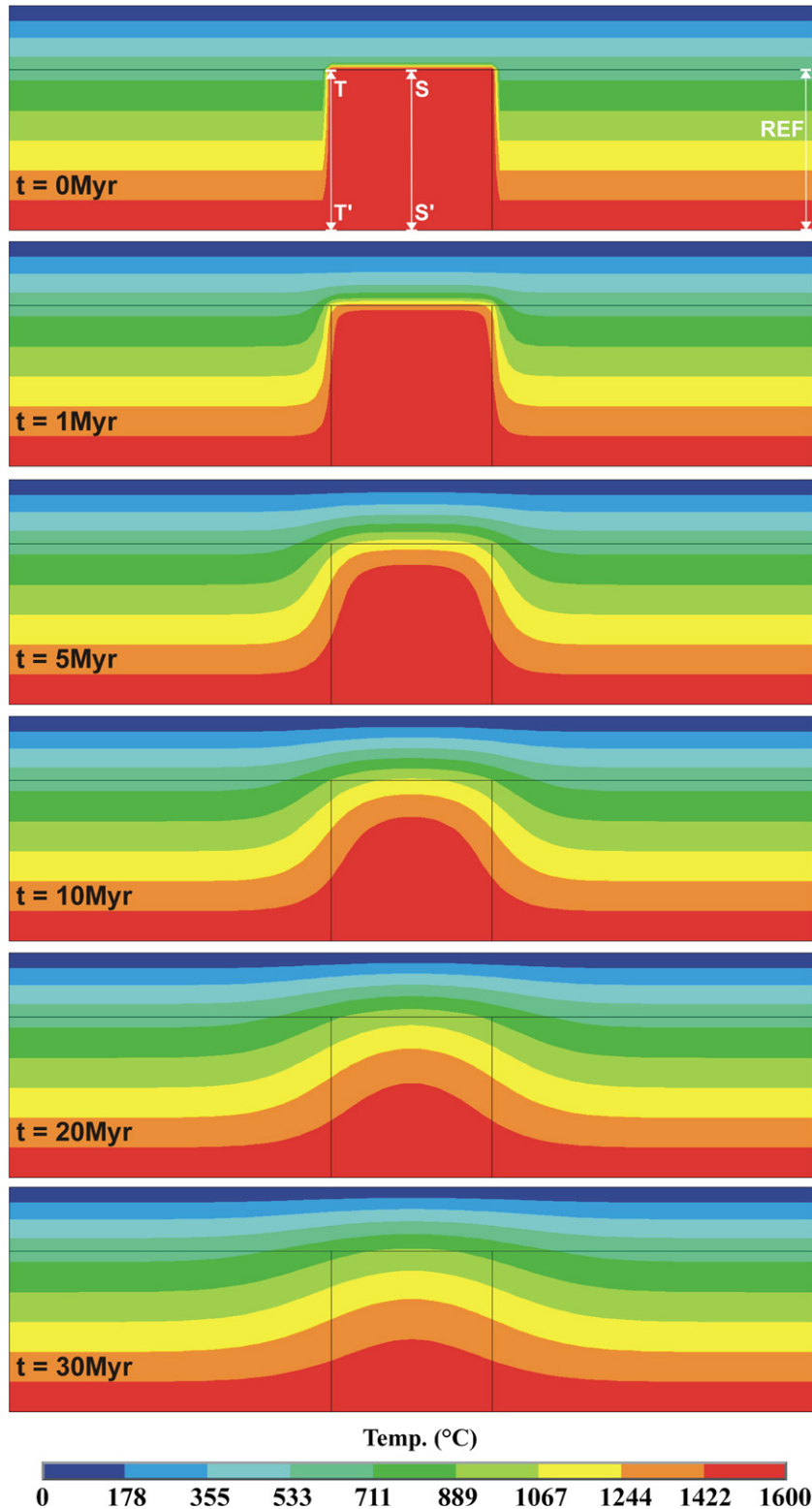


Fig. 8. 2D finite-element model: thermal evolution after impingement of an asthenospheric diapir at 40 km depth at $t = 0$. The temperature of the diapir is initially $T_d = 1600$ °C and it is allowed to evolve. Note the fast decay in diapir temperature and the progressive increase of temperatures above and aside it. REF, SS' and TT' are vertical profiles used to sample mantle densities in order to compute the evolution of density contrasts existing between the diapir and the surrounding lithospheric mantle (see text for details).

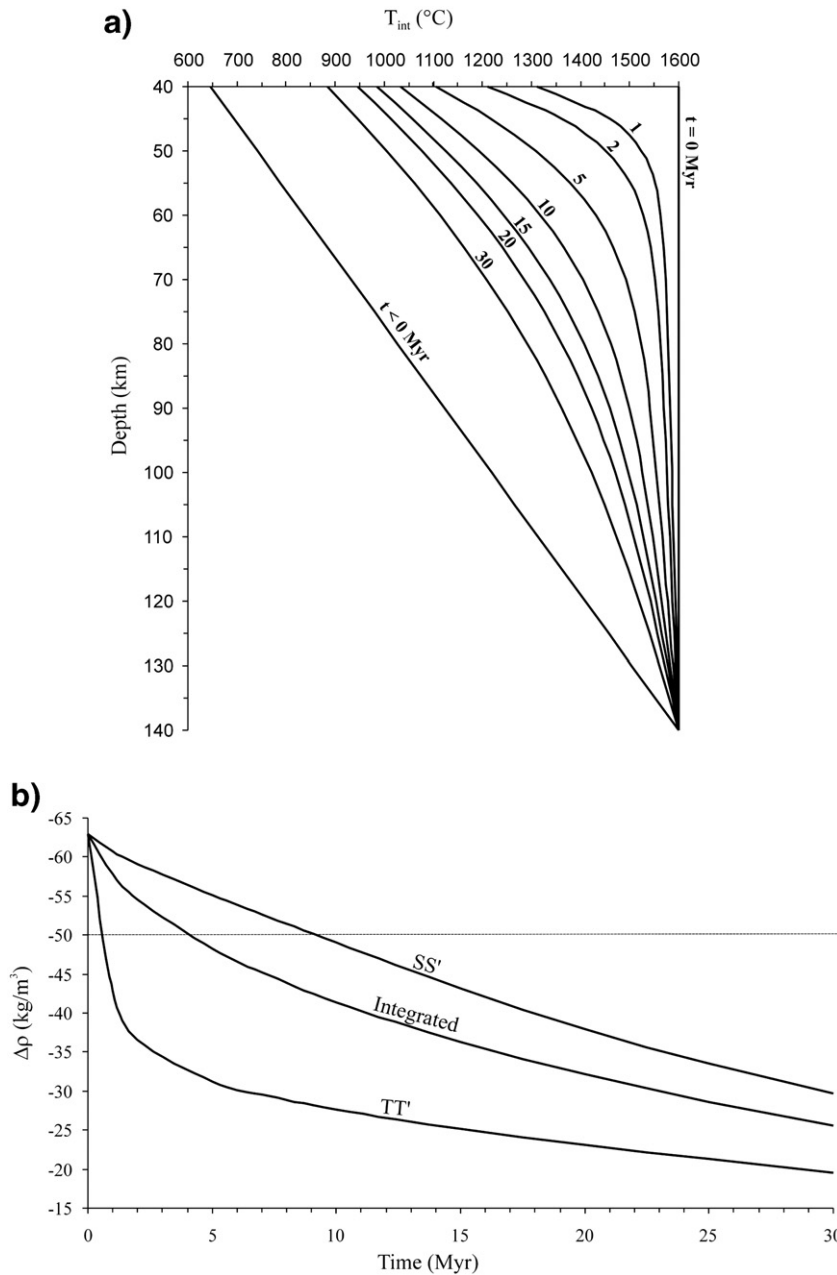


Fig. 9. Results from the 2D finite-element model shown in Fig. 8. a) Temperature evolution at the lateral edges of the asthenospheric diapir (TT' profile). Labels indicate time in Myr after diapir emplacement, $t < 0$ Myr represents the situation before diapir impingement the system is returning to. b) Density contrast existing between the diapir and the surrounding lithosphere. SS' and TT' indicate the vertical profiles for which densities were calculated. The curve "Integrated" represents the evolution of the average density contrast (see text for details).

$\Delta q \sim 23 \text{ mW/m}^2$ at $t \sim 15$ Myr. Therefore, assuming that no magma has reached relatively shallow levels in the crust, the heat flow anomaly would not be detectable despite the extremely high temperature assumed for the mantle diapir.

As temperatures decline within the diapir, its density increases. Using modelled temperatures and Eq. (1), we computed the evolution of the density contrast between asthenospheric rocks within the diapir and the surrounding mantle lithosphere ($\Delta\rho$, Fig. 9b). The average density of the mantle lithosphere was computed by integrating densities along a vertical profile at $t = 0$ (i.e. vertical profile REF on Fig. 8) and was used as reference density in order to calculate $\Delta\rho$ values. Two curves for the evolution of $\Delta\rho$ were built using integrated densities along (1) vertical profile SS', giving maximum density contrasts (i.e. slowest cooling by the middle of the diapir, Fig. 8) and (2) vertical profile TT', giving minimum density contrasts (i.e. fastest

cooling at the edge of the diapir, Fig. 8). The third curve (i.e. "Integrated" in Fig. 9b) represents the evolution of the average $\Delta\rho$ and was constructed by integrating density values over the total area occupied by the diapir (Fig. 7). Note that the $\Delta\rho$ values computed here represent uppermost bounds. This is because lithosphere mantle rocks become lighter than they were initially as the thermal wave progresses outside the diapir.

The results show that densities increase extremely fast at the lateral edges of the diapir (i.e. TT' curve in Fig. 9b, $+20 \text{ kg/m}^3$ between 0 and 1 Myr) whereas the density increase is much slower at its central profile (i.e. SS' curve). In addition, Fig. 9b shows that "Integrated" $\Delta\rho$ values drop below -50 kg/m^3 (e.g. the uppermost value required in order to explain the observed Bouguer anomaly, Fig. 5) shortly after ~ 4 Myr and reach -25 kg/m^3 at $t = 30$ Myr. Our results imply that the topography of the southern Scandes should have decayed significantly after the

hypothetical intrusion of an asthenospheric diapir at shallow depths in the lithosphere 30 Myr ago. Furthermore, the density contrast between the diapir and the lithosphere, 30 Myr after the emplacement of the diapir, is much too modest to account for the gravity low below the southern Scandes. The evident conclusion from this modelling exercise is that the southern Scandes are not isostatically balanced by an asthenospheric diapir at depth.

4. Discussion and conclusions

Our integrated gravity/thermal approach demonstrates that the topography of the southern Scandes is not compensated by a mantle thermal anomaly at depth. A simple analysis of the Bouguer gravity field shows that the mass deficit needs to be located close to the Moho as already demonstrated by Olesen et al. (2002). New heat flow data show that whatever the nature of this mass deficit it cannot, in any case, be related to a thermal anomaly. This statement would find even more support if we would have considered thermal advection in our computations, which is a far more efficient and, perhaps, more natural way to transport excess of heat to the surface.

A recent passive seismic experiment suggests that the crust thickness at the location of the highest mountains of southern Norway (i.e. Jotunheimen) is 4–5 km more than anticipated (Svenningsen et al., 2007). The authors of this study show that the updated crustal configuration can explain the observed gravity signal and argue that the Scandes are compensated by an Airy-type “crustal root”. The apparently low rigidity characterising the lithosphere of southern Norway (Rohrman et al., 2002; Ebbing and Olesen, 2005; Pérez-Gussinyé and Watts, 2005; Pascal and Cloetingh, 2009) would indeed favour local isostasy and the regions with the thickest crust would naturally be the most elevated. However, in general no firm correlation can be seen between the seismically determined Moho and the observed topography (e.g. Ebbing and Olesen, 2005). This suggests that the topography is merely compensated by a mixture of different sources including Pratt-like lateral variations in density in the crust and/or in the mantle. For example, Olesen et al. (2002) showed by means of isostasy/gravity modelling that the rugged topography of the northern Scandes is compensated to a large degree by mass deficit in the crust itself. In brief, there is an absolute need to sort out the mechanisms responsible for the uplift and those that sustain present-day topography.

We stress that our analysis does not inform on what caused uplift of the Scandes. Indeed the only criticism that can be addressed to Rohrman and van der Beek's theory holds on the assumption that the Bouguer gravity low associated to the Scandes reflect the signal produced by an asthenospheric diapir or, conversely, that the present-day topography is compensated by such a mantle thermal anomaly. The other arguments in favour of their model appear to remain valid. In particular, the existence of a low-velocity anomaly at 75–150 km depth below southern Norway has been confirmed by a very recent tomographic study (Weidle and Maupin, 2008). This study was able to resolve the mantle structure of the NE Atlantic with a much better resolution than previous seismic studies (Husebye et al., 1986; Bannister et al., 1991; Rohrman et al., 2002) and imaged a continuous low-velocity anomaly stretching from Iceland to southern Norway as proposed in the asthenospheric diapir model.

All this calls for a modification but surely not a complete rejection of Rohrman and van der Beek's theory. With the data currently at hand, our working hypothesis is the following. Hot asthenosphere was channelled from Iceland or from the mid-oceanic ridges to the Fennoscandian Shield in the way described by Rohrman and van der Beek (1996). Interaction between asthenosphere and cratonic lithosphere did not produce a Rayleigh–Taylor instability, perhaps because the NE-Atlantic asthenosphere is not as hot as previously claimed. Instead, warming of the southern Norway lithosphere could have resulted in progressive reduction of its bulk density and of its rigidity

and, finally, modest uplift of the surface as already suggested by Nielsen et al. (2002). Erosion, enhanced by late Cenozoic climatic deterioration, amplified the topography and produced the final shape and altitude of the present-day Scandes.

Acknowledgements

The ideas expressed in this paper have been matured in the course of the KONTIKI (*Continental Crust and Heat Generation in 3D*) and HeatBar (*Basement Heat Generation and Heat Flow in the western Barents Sea, Petromaks project nr. 169438*) projects financed by StatoilHydro and the Research Council of Norway. We express our warm thanks to Niels Balling and an anonymous reviewer for their accurate and constructive reviews that helped to improve the present paper significantly.

References

- Afonso, J.C., Ranalli, G., Fernandez, M., 2005. Thermal expansivity and elastic properties of the lithospheric mantle: results from mineral physics of composites. *Physics of the Earth and Planetary Interiors* 149, 279–306.
- Balling, N., 1980. The land uplift in Fennoscandia, gravity field anomalies and isostasy. In: Mörner, N.-A. (Ed.), *Earth Rheology, Isostasy and Eustasy*. John Wiley & Sons, New York, pp. 297–321.
- Bannister, S.C., Ruud, B.O., Husebye, E.S., 1991. Tomographic estimates of sub-Moho seismic velocities in Fennoscandia and structural implications. *Tectonophysics* 189, 37–53.
- Bodell, J.M., Chapman, D.S., 1982. Heat flow in the North-Central Colorado Plateau. *Journal of Geophysical Research* 87, 2869–2884.
- Carslaw, H.S., Jaeger, J.C., 1959. *Conduction of Heat in Solids*. Oxford University Press, London, 386 pp.
- Cloetingh, S.A.P.L., Gradstein, F.M., Kooi, H., Grant, A.C., Kaminski, M., 1990. Plate reorganization; a cause of rapid late Neogene subsidence and sedimentation around the North Atlantic. *Journal Geological Society of London* 147, 495–506.
- Dehls, J.F., Olesen, O., Bungum, H., Hicks, E., Lindholm, C.D., Riis, F., 2000. Neotectonic map, Norway and adjacent areas 1:3 mill. *Norges geologiske undersøkelse*, Trondheim, Norway.
- Doré, A.G., 1992. The base Tertiary surface of southern Norway and the northern North Sea. *Norsk Geologisk Tidsskrift* 72, 259–265.
- Ebbing, J., Olesen, O., 2005. The northern and southern Scandes – structural differences revealed by an analysis of gravity anomalies, the geoid and regional isostasy. *Tectonophysics* 411, 73–87.
- Ebbing, J., Afework, Y., Olesen, O., Nordgulen, Ø., 2005. Is there evidence for magmatic underplating beneath the Oslo Rift? *Terra Nova* 17, 129–134.
- Eyles, N., 1996. Passive margin uplift around the North Atlantic and its role in Northern Hemisphere late Cenozoic glaciation. *Geology* 24, 103–106.
- Faleide, J.J., Kyrkjebø, R., Kjennerud, T., Gabrielsen, R., Jordt, H., Fanavoll, S., Bjerke, M.D., 2002. Tectonic impact on sedimentary processes during Cenozoic evolution of the northern North Sea and surrounding areas. In: Doré, A.G., Cartwright, J.A., Stoker, M.S., Turner, J.P., White, N. (Eds.), *Exhumation of the North Atlantic Margin: Timing, Mechanisms and Implications for Petroleum Exploration*. Special Publications – Geological Society of London, vol. 196, pp. 235–269.
- Goes, S., Cammarano, F., Hansen, U., 2004. Synthetic seismic signature of thermal mantle plumes. *Earth and Planetary Science Letters* 218, 403–419.
- Husebye, E.S., Hovland, J., Christofferson, A., Åström, K., Slunga, R., Lund, C.E., 1986. Tomographic mapping of the lithosphere and asthenosphere beneath Southern Scandinavia and adjacent areas. *Tectonophysics* 28, 229–250.
- Hänel, R., Grønlie, G., Heier, K.S., 1979. Terrestrial heat-flow determination in Norway and an attempted interpretation. In: Cermak, V., Rybach, L. (Eds.), *Terrestrial Heat Flow in Europe*. Springer-Verlag, Berlin, pp. 232–240.
- Japsen, P., Chalmers, J.A., 2000. Neogene uplift and tectonics around the North Atlantic: Overview. *Global and Planetary Change* 24, 165–173.
- Kinck, J.J., Husebye, E.S., Larsson, F.R., 1993. The Moho depth distribution in Fennoscandia and the regional tectonic evolution from Archean to Permian times. *Precambrian Research* 64, 23–51.
- Korhonen, J.V., Aaro, S., All, T., Elo, S., Haller, L.A., Kääriäinen, J., Kulnich, A., Skilbrei, J.R., Solheim, D., Säävuori, H., Vaher, R., Zhdanova, L., Koistinen, T., 2002. Bouguer anomaly map of the Fennoscandian shield 1: 2,000,000. Geological Surveys of Finland, Norway and Sweden and Ministry of Natural Resources of Russian Federation.
- Lawver, L.A., Müller, R.D., 1994. Iceland hotspot track. *Geology* 22, 311–314.
- Lidmar-Bergström, K., Näslund, J.O., 2002. Landforms and uplift in Scandinavia. Special Publication – Geological Society of London, vol. 196. Geological Society, London, pp. 103–116.
- Milnes, A.G., Koestler, A.G., 1985. Geological structure of Jotunheimen, southern Norway (Sognefjell-Valdres cross-section). In: Gee, D.G., Sturt, B.A. (Eds.), *The Caledonide Orogen—Scandinavia and Related Areas*. Wiley, Chichester, pp. 457–474.
- Nielsen, S.B., Paulsen, G.E., Hansen, D.L., Gemmer, L., Clausen, O.R., Jacobsen, B.H., Balling, N., Huuse, M., Gallagher, K., 2002. Paleocene initiation of Cenozoic uplift in Norway. In: Doré, A.G., Cartwright, J.A., Stoker, M.S., Turner, J.P., White, N. (Eds.), *Exhumation of the North Atlantic Margin: Timing, Mechanisms and Implications for Petroleum Exploration*. Special Publications – Geological Society of London, vol. 196, pp. 45–65.
- Nielsen, S.B., Gallagher, K., Leighton, C., Balling, N., Svenningsen, L., Jacobsen, B.H., Thomsen, E., Nielsen, O.B., Heilmann-Clausen, C., Egholm, D.L., Summerfield, M.A.,

- Clausen, O.R., Piotrowski, J.A., Thorsen, M.R., Huuse, M., Abrahamsen, N., King, C., Lykke-Andersen, H., 2009. The evolution of western Scandinavian topography: A review of Neogene uplift versus the ICE (isostasy-climate-erosion) hypothesis, *Journal of Geodynamics* 47, 72–95.
- Nyblade, A.A., Pollack, H.N., 1993. A global analysis of heat flow from Precambrian terrains: implications for the thermal structure of Archean and Proterozoic lithosphere, *Journal of Geophysical Research* 98, 12207–12218.
- Olesen, O., Lundin, E., Nordgulen, Ø., Osmundsen, P.T., Skilbrei, J.R., Smethurst, M.A., Solli, A., Bugge, T., Fichler, C., 2002. Bridging the gap between the onshore and offshore geology in Nordland, northern Norway. *Norwegian Journal of Geology* 82, 243–262.
- Pascal, C., Cloetingh, S.A.P.L., 2009. Gravitational potential stresses and stress field of passive continental margins: insights from the south-Norway shelf. *Earth & Planetary Science Letters* 277, 464–473.
- Pérez-Gussinyé, M., Watts, A.B., 2005. The long-term strength of Europe and its implications for plate forming processes. *Nature* 436. doi:10.1038/nature03854.
- Poudjom Djomani, Y.H., O'Reilly, S.Y., Griffin, W.L., Morgan, P., 2001. The density structure of subcontinental lithosphere through time. *Earth and Planetary Science Letters* 184, 605–621.
- Rasmussen, R., Pedersen, L.B., 1979. End corrections in potential field modeling. *Geophysical Prospecting* 27, 749–760.
- Redfield, T.F., Osmundsen, P.T., Hendriks, B.W.H., 2005. The role of fault reactivation and growth in the uplift of western Fennoscandia. *Journal of the Geological Society, London* 162, 1–18.
- Reusch, H., 1901. Nogle bidrag till forstaaelsen af hvorledes Norges dale og fjelde er blevne til. *Norges Geologiske Undersøkelse* 32, 124–263.
- Reusch, H., 1903. Betrachtungen über das Relief von Norwegen. *Geographische Zeitschrift* 9, 425–435.
- Riis, F., 1996. Quantification of Cenozoic vertical movements of Scandinavia by correlation of morphological surfaces with offshore data. *Global and Planetary Change* 12, 331–357.
- Riis, F., Fjeldskaar, W., 1992. On the magnitude of the Late Tertiary and Quaternary erosion and its significance for the uplift of Scandinavia and the Barents Sea. *Special Publication — Norwegian Petroleum Society* 1, 163–185.
- Rohrman, M., van der Beek, P., 1996. Cenozoic postrift domal uplift of North Atlantic margins; an asthenospheric diapirism model. *Geology* 24, 901–904.
- Rohrman, M., van der Beek, P.A., Andriessen, P.A.M., Cloetingh, S.A.P.L., 1995. Meso-Cenozoic morphotectonic evolution of southern Norway: Neogene domal uplift inferred from apatite fission track thermochronology. *Tectonics* 14, 704–718.
- Rohrman, M., van der Beek, P.A., van der Hilst, R.D., Reemst, P., 2002. Timing and mechanisms of North Atlantic Cenozoic Uplift: Evidence for mantle upwelling. In: Doré, A.G., Cartwright, J.A., Stoker, M.S., Turner, J.P., White, N. (Eds.), *Exhumation of the North Atlantic Margin: Timing, Mechanisms and Implications for Petroleum Exploration*. Special Publications — Geological Society of London, pp. 27–43.
- Sales, J.K., 1992. Uplift and subsidence of northwestern Europe: possible causes and influence on hydrocarbon productivity. *Norsk Geologisk Tidsskrift* 72, 253–258.
- Skelton, A., Jakobsson, M., 2007. Could peridotite hydration reactions have provided a contributory driving force for Cenozoic uplift and accelerated subsidence along the margins of the North Atlantic and Labrador Sea? *Norwegian Journal of Geology* 87, 21–28.
- Skilbrei, J.R., 1990. Structure of the Jotun Nappe Complex, southern Norwegian Caledonides: ambiguity of gravity modelling and reinterpretation. *Geological Survey of Norway Report* 89.169. 26 pp.
- Skilbrei, J.R., Kihle, O., Olesen, O., Gellein, J., Sindre, A., Solheim, D., Nyland, B., 2000. Gravity anomaly map Norway and adjacent ocean areas, scale 1:3 Million, Geological Survey of Norway, Trondheim.
- Slagstad, T., Balling, N., Elvebakk, H., Middtomme, K., Olesen, O., Pascal, C., in revision. Heat-flow measurements in early Mesoproterozoic to Permian geological provinces in south and central Norway and a new heat-flow map of Fennoscandia and the Norwegian–Greenland Sea. Submitted to *Tectonophysics*.
- Stuevold, L.M., Eldholm, O., 1996. Cenozoic uplift of Fennoscandia inferred from a study of the mid-Norwegian margin. *Global and Planetary Change* 12, 359–386.
- Svenningsen, L., Balling, N., Jacobsen, B.H., Kind, R., Wylegalla, K., Schweitzer, J., 2007. Crustal root beneath the highlands of southern Norway resolved by teleseismic receiver functions. *Geophysical Journal International* 170, 1129–1138.
- Talwani, M., Worzel, J.L., Landisman, M., 1959. Rapid gravity computations for two-dimensional bodies with application to the Mendocino submarine fracture zone. *Journal of Geophysical Research* 64, 49–59.
- Torske, T., 1972. Tertiary oblique uplift of western Fennoscandia, crustal warping in connection with rifting and break up of the Laurasian continent. *Norges Geologiske Undersøkelse* 273, 43–48.
- Weidle, C., Maupin, V., 2008. An upper mantle S-wave velocity model for Northern Europe from Love and Rayleigh group velocities. *Geophysical Journal International* 175, 1154–1168.